JSST
Journal of Space Science & Technology

Vol. 7/ No. 1/ 2014
pp. 33-40

Laminar and Turbulent Aero Heating Predictions over Blunt Body in Hypersonic Flow

S. A. Hosseini[1*] and S. Noori[2]

1, 2. Astronautic Research Institute, Iranian Space Research Center

2. Department of Aerospace Engineering, Center of Excellence in Computational Aerospace Engineering, Amirkabir University of Technology

[*]Postal Code: 1465774111, Tehran, IRAN

Hosseini@ari.ac.ir

In the present work, an engineering method is developed to predict laminar and turbulent heating-rate solutions for blunt reentry spacecraft at hypersonic conditions. The calculation of aerodynamic heating around blunt bodies requires alternative solution of inviscid flow field around the hypersonic bodies. In this paper, the procedure is of an inverse nature, that is, a shock wave is assumed and calculations proceed along rays normal to the shock. The solution is iterated until the given body is computed. The inverse method is practical for the calculation of flow field between the shock wave and the body surface. Body calculation with the body analysis is contrasted and according to the entire differences between those; the shape of shock with the coefficient scales is implemented. The normal momentum equation is replaced with a Maslen's second order pressure equation. This simplification significantly decreases machine computation time. The present method predicts laminar and turbulent heating-rates that compare favorably with other researches. Since the method is very high-speed, it can be used for preliminary design, or parametric study of aerodynamics vehicles and thermal protection of hypersonic flows.

Keywords: Aerodynamic heating, blunt body, hypersonic flow, flow field, turbulent flow, laminar flow

Nomenclature

a	major axis of ellipse $\frac{a}{l}$
b	minor axis of ellipse $\frac{b}{l}$
l	Characteristic length
M_∞	Free-stream Mach number
$\rho(\psi)$	pressure through shock layer
R_b, R_{st}	body radius of curvature at stagnation point
r	cross- sectional radius
U_∞	Free-stream velocity
u	Shock layer velocity in x-direction
u_s	velocity behind shock in x-direction
v	shock velocity in y-direction
v_s	velocity behind shock in y-direction
x	coordinate measured along shock wave from axis of symmetry
y	coordinate normal to shock
Z_b	coordinate measured along axis of symmetry
Z_s	value of z for shock point
$\theta_{\gamma b}$	Ratio of specific heats
θ_s	Shock angle
θ_b	Body angle
ρ_∞	Free-stream density
ψ	Local stream function through shock layer
H	total enthalpy
q	Convection heating

1. M. Sc. (Corresponding Author)
2. Assistant Professor

Introduction

The preliminary thermal design of hypersonic vehicles requires accurate and reliable prediction of the convective heating over the blunt nose of the vehicle. Since aerodynamic heating is a function of V_∞^3, its consideration in hypersonic flights is more important than aerodynamic forces. Therefore, in high speeds the first concern is the large amount of heat production on the surface of vehicle which highly increases the shell temperature. Often approximate methods, which have

Recived: 2011.11.13 , Accepted: 2014.03.03

been proven by experimental data and/or "bench mark" calculations, are employed in parametric or design calculations. Nevertheless, the current interest in outer-planet entry and advanced-transportation systems for the Earth entry has resulted in additional problems for convective-heating analyses.

Such results may be obtained by numerically solving the Navier- Stokes (NS) equations [1, 2], or one of their various subsets such as the parboiled Navier-Stokes (PNS) [3-5], and viscous shock layer (VSL) equations [6-9], for the flow field surrounding the vehicle, but these methods require extensive computer run times and storage, and are not generally applicable to parametric studies or preliminary design calculations.

Two of the simpler engineering aerodynamic heating methods currently used are AROHEAT [10-13], and INCHES [14]. AEROHEAT calculates approximate surface streamlines based solely on the body geometry, and assumes modified Newtonian theory which is inaccurate for slender bodies; while INCHES uses an approximate expression for the scale factor in the windward and lee ward planes which describes the spread of surface streamlines and assumes an axisymmetric Maslen technique. Another approximate solution for convection heating rate is LATCH (Langley Approximate Three dimensional Convective Heating) code [15] which provides reasonably accurate heating rates over most of the re-entry vehicles.

The other important activities performed in the field of calculating aerodynamic heating resulted in an approximate inviscid method by Riley and Dejarnette in 1992[16]. As this method is suitable for the primary design, the method used in this article is base on the method of ref 16.

In this paper an approximate method has been developed for solving the Aerodynamic heating around re-entry vehicle. This method is an inverse nature, which a shock wave is assumed and calculations are preceded between the shock and body, to calculate all properties after the shock. For simplicity the normal momentum equation is replaced with a second order pressure relation; this simplification significantly reduces computation time. On the other hand, used to the commercial CFD code for flow field solution. The numerical simulations are able to generate large amount of data that describes the fluid flow, using information from every node and every cell of the grid that models the fluid domain. So, since the grid is sufficiently dense, unstructured mesh, the flow can be reconstructed and the flow features extracted and analyzed. To predict laminar and turbulent surface heating rates, Zoby's convective-heating approximate equation has been used [18]. The method provides a rapid technique such as spherically and ellipsoid. An excellent agreement is observed between the results obtained in this paper and those calculated by other research. Since the method is very fast it can be used for preliminary design, or parametric study of vehicle aerodynamics at hypersonic flows.

Governing Equations and Method of Solution

This section describes an inviscid method solution in conjunction with the procedure for computing inviscid flow with the assumption that the flow field is axisymmetric and that the shock layer is thin. The equations, for this method, are written in a perpendicular curvilinear coordinate system fixed at the axis of symmetry of the shock (See Figure 1).

The governing equations with upside descriptions follow:

Continuity:

$$\left(\frac{\partial(r^n\rho u)}{\partial x}\right)_y + \left(\frac{\partial(r^n\rho v)}{\partial y}\right)_x = 0 \quad (1)$$

X-momentum:

$$u(\frac{\partial u}{\partial x})_y + v(\frac{\partial u}{\partial y})_x - \frac{uv}{R_s} = -\frac{1}{\rho}(\frac{\partial P}{\partial x})_y \quad (2)$$

Y-momentum:

$$u(\frac{\partial v}{\partial x})_y + v(\frac{\partial v}{\partial y})_x + \frac{u^2}{R_s} = -\frac{1}{\rho}(\frac{\partial P}{\partial y})_x \quad (3)$$

Entropy:

$$u(\frac{\partial s}{\partial x})_y + v(\frac{\partial s}{\partial y})_x = 0 \quad (4)$$

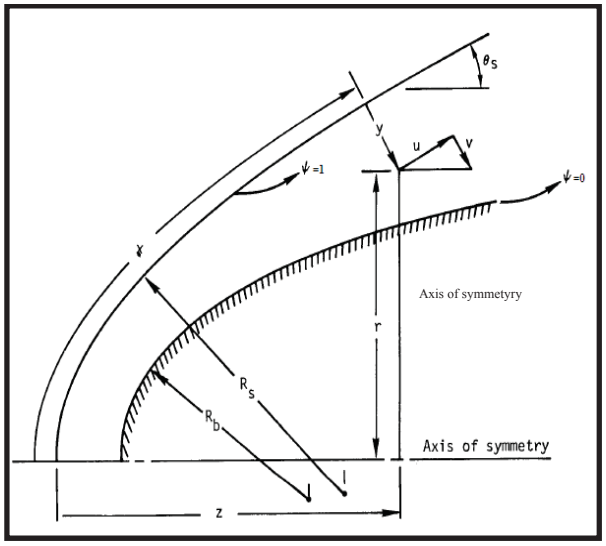

Fig. 1 Sketch coordinate system

In this paper, the procedure is of an inverse nature that is assuming a shock-wave shape (Figure.1). Maslen's method is an inverse method, where a shock wave is assumed and calculations proceeded along rays

normal to the shock somewhere between $0 < \psi < 1$. The solution is iterated until the given body is computed. The inverse method is applied for the calculation of flow field between the shock wave and the body surface. Calculation body is contrasted with the analysis bodyand according to the entire errors between them the shape of shock with the coefficient scales are approved.

The analysis developed by Maslen will be outlined as an example of theory based on the assumption of a thin shock layer (the normal momentum equation is replaced with Maslen's second order pressure equation). A Von-Mises transformation [16] is introduced so that the independent variables are the distance along the shock (x) and the stream function (ψ)[17].

$$\frac{\partial \psi}{\partial y} = -\mathrm{r^n}\rho u \tag{5}$$

$$\frac{\partial \psi}{\partial \mathrm{x}} = \mathrm{r^n}\rho v \tag{6}$$

If these transformations are applied to the y-momentum equation, this equation becomes:

$$r^{\mathrm{n}} \frac{\partial P}{\partial \psi} = \frac{u}{R_s} + (\frac{\partial v}{\partial x})_{\psi} \tag{7}$$

In the analysis of Maslen, he assumed that $(\frac{\partial v}{\partial x})_{\psi}$ is very small and that the streamlines are nearly parallel to the shock, $u \approx u_s$,(u_s is the velocity behind the shock). Thus, equation (7) becomes:

$$(\frac{\partial s}{\partial x})_{\psi} = 0 \tag{8}$$

Integrating equation (8) between a point in the shock layer where the value of the stream function is ψ and just behind the shock wave where $\psi = \psi_s$, we have:

$$P(\psi) = P_s + \frac{u_s}{r_s^n R_s}(\psi - \psi_s) \tag{9}$$

Equation (9) is Maslen's second order pressure.

With the effects of the normal velocity gradients included in equation (9), an approximation to the normal velocity component is necessary.

$$V(\psi) = \mathrm{V_s} + \frac{\psi}{\psi_s} \tag{10}$$

Preliminary calculations indicate that equation (10) is satisfactory as an initial guess for the normal velocity profile, but better agreement is obtained with the existing results if the normal velocity component is reevaluated during each iteration [14]

$$V(\psi) = \mathrm{V_s} + \frac{[1-\frac{\mathrm{y}(\psi)}{\mathrm{yt}}]^{1/2}}{1-\frac{\mathrm{y}(\psi)}{\mathrm{R_S}}} \tag{11}$$

Calculating the velocity from the adiabatic energy equation (total enthalpy is constant), that is,

$$h_0 = h_\infty + \frac{V_\infty^2}{2} \tag{12}$$

Where h_0 is the total enthalpy, which is constant throughout the adiabatic flow field. In turn,

(ignoring$v$)

$$u_2 = \sqrt{2(h_0 - h_2)} \tag{13}$$

The y-coordinate is computed using the equation, through the flow field geometry (Figure 1).

$$r = r_s - y\cos\theta_s \tag{14}$$

Replacing equation (14) with equation (5) and solving that for y gives:

$$y = \frac{r_s}{\cos\theta_s}\left[1 - \left(1 - \frac{2\cos\theta_s}{r_s^2}\int_{\psi}^{\psi_s}\frac{1}{\rho u}d\psi\right)^{1/2}\right] \tag{15}$$

Comparisons of the present results with the shock shapes and surface pressure distributions obtained by the more exact methods indicate that the program provides reasonably accurate results for smooth bodies in the axisymmetric flow. The geometries specified in the program are spherical and ellipsoid.

Aerodynamic Heating Calculations

Zoby's approximate convective heating equations [18] are obtained from the integral form of the axisymmetric boundary layer momentum equation [19]. The equations for laminar flow are as follows [20] :

$$q_{wl} = 0.22(Re_{\theta l})^{-1}(\frac{\rho^*}{\rho_e})(\frac{\mu^*}{\mu_e})\rho_e u_e(h_{aw} - h_w)(Pr_w)^{-0.6} \tag{16}$$

The variable of ρ^* and μ^* are introduced to consider the compressibility effects. These variables are evaluated at the Eckert's reference enthalpy [21] defined as:

$$H^* = 0.50\, H_e + 0.50\, H_w + 0.22R\frac{V_e^2}{2} \tag{17}$$

The laminar boundary layer momentum thickness is:

$$\theta_l = \frac{0.664(\int_0^{\xi^-}\rho^*\mu^* u_e h_{\beta^-} d\xi^-)^{\frac{1}{2}}}{\rho_e u_e h_{\beta^-}} \tag{18}$$

The adiabatic wall enthalpy is defined as:

$$H_{aw} = H_e + 0.5RV_e^2 \tag{19}$$

Similar equations are developed for the turbulent flow [15]:

$$q_{wT} = C_l(Re_{\theta T})^{-m}(\frac{\rho^*}{\rho_e})(\frac{\mu^*}{\mu_e})^m \rho_e u_e(h_{aw} - h_w)(Pr_w)^{-0.4} \quad (20)$$

The Turbulent boundary layer momentum thickness is:

$$\theta_T = \frac{(C_2 \int_0^{\xi^-} \rho^* \mu^{*m} u_e h_{\beta^-}{}^{C_3} d\xi^-)^{C_4}}{\rho_e u_e h_{\beta^-}} \quad (21)$$

The coefficients of m, C_1, C_2, C_3 and C_4 are functions of N and experimental results [18] and show that N would be a function of $Re_{\theta T}$, and are obtained by:

$$C_4 = \frac{1}{C_3} \quad (22)$$

$$m = \frac{2}{N+1}$$

$$C_3 = 1 + m$$

$$C_5 = 2.2433 + 0.93N \quad (23)$$

$$C_1 = \left(\frac{1}{C_5}\right)^{\frac{2N}{N+1}} \left[\frac{N}{(N+1)(N+2)}\right]^m \quad C_2 = (1+m)c_1 \quad (24)$$

$$N = 12.67 - 6.5log(Re\theta_T) + 1.21[log(Re\theta_T)]^2 \quad (25)$$

The values of pressure, temperature, density and the velocity magnitude at the edge of the boundary (i.e. P_i, T_e, ρ_i and V_i) are calculated from the present method and commercial CFD codes. For perfect gas model, the viscosity is obtained using the Sutherland formula [19], and the specific heat ratio and Prandtl number are assumed to be constants of 1.4 and 0.71, respectively.

Results

The numerical results of this method are compared with those obtained from the experiment and other numerical data. The method provides a rapid technique similar to spheres and ellipsoids.

The Shock wave shape over a spherically blunted nose for M_∞ =10 and γ = 1.66 is shown in Figure 2. The results obtained from the present approach are compared with those of ref.22. Good agreement between the results of the present method and experimental data is shown in Figure 2. The pressure distribution over spherically blunted nose is also shown Figure 3. These results are compared with pressure distribution and shock shape, ref 22 and ref 23. In this comparison, there is an error of less than 10% noted. This difference is due to the assumed method. The commercial CFD code output results are shown in Figure 4 and Figure 5. These figures are related to contours of Mach and temperature.

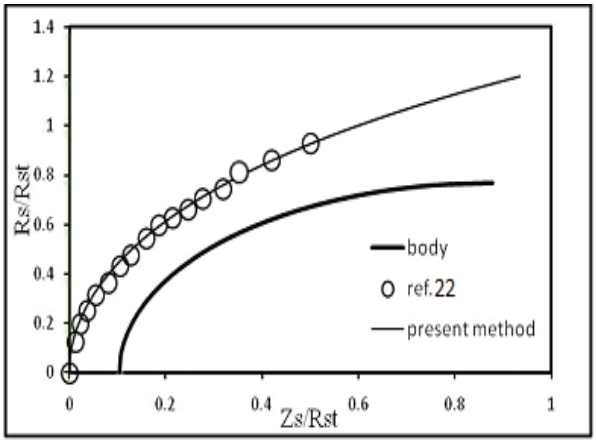

Fig. 2 Sphere shock shape sphere at M_∞=10 and γ=1.66, R_{st}=1.43

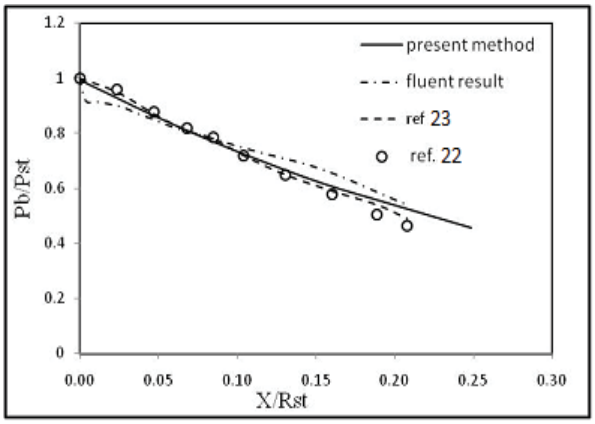

Fig. 3 Pressure distribution on sphere at $M_\infty = 10$ and $\gamma = 1.66$. $R_{st} = 1.43$

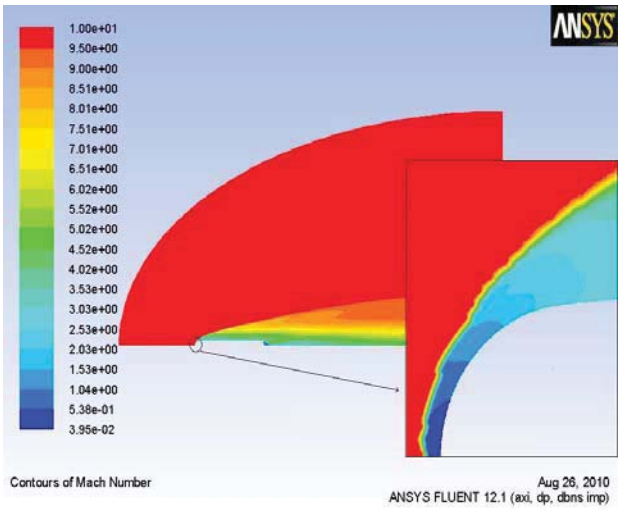

Fig. 4 Contours of Mach number for sphere at M_∞=10 and γ=1.66, R_{st}=1.43

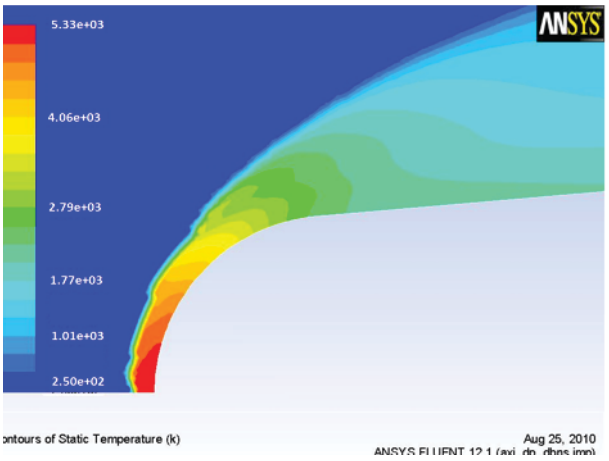

Fig. 5 Contours of temperature sphere at $M_\infty=10$ and $\gamma=1.66$, $R_{st}=1.43$

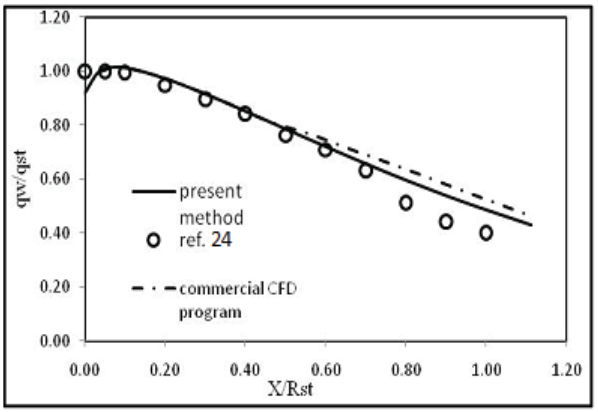

Fig. 6 Convection heating distribution on sphere at $T_W = 430$

The turbulent convection heating rate over a spherically blunted nose for and M_∞ =10 and γ = 1.66 are shown in Figure 6. By comparing the present method and ref 23, a good agreement can be observed between them (less than 10% disagreement). Also comparison between the results of the present method and commercial CFD code data is depicted in Figure 6 (within 10%). The maximum value obtained by aerodynamic heating on the nose is (49343.44 MW/m^2). The shock shape and pressure distribution over a spherically blunted nose for M_∞ =15 and γ = 1.4 are shown in Figures 7 and 8. These results compare with shock wave shape and pressure distribution ref 22. The good agreement is also observed between the present method and the published result of ref 22 (less than 10% disagreement).

Computed laminar surface heating rates are presented in Figure 9 for a 5-deg spherically blunted cone at zero angle of attack .The free streams Mach number is 15 and the wall temperature is 266'k. Results of the present method and ref 24 are shown in Figure 9. Generally, good agreement is also obtained for heating rate comparisons with a maximum discrepancy of approximately 12%. In Figure 10 and 11 contours of temperature and Mach number can be seen. These figures are related to the commercial CFD program output. The maximum q_{st} in Figure 9 is 56545.44 (MW/m^2).

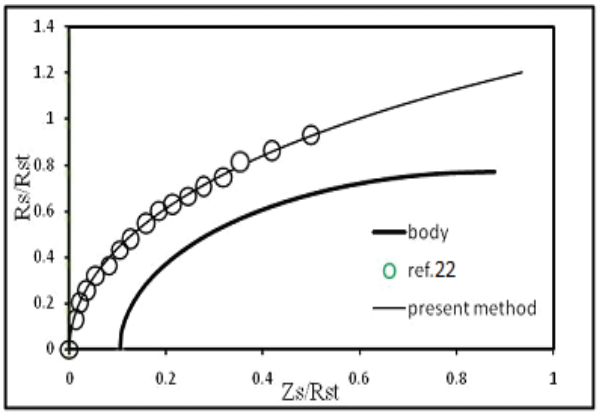

Fig. 7 Sphere shock shape at $M_\infty=15$ and $\gamma=1.4$

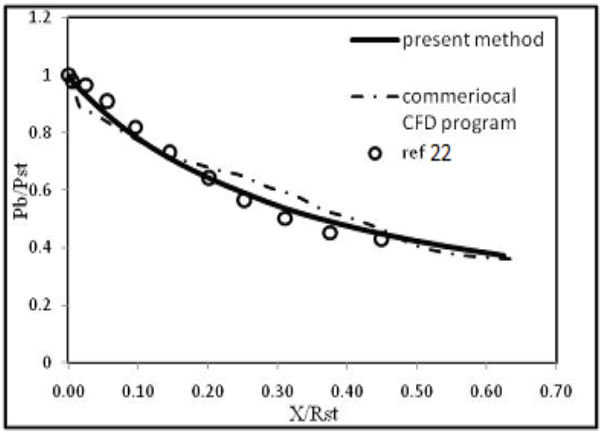

Fig. 8 Pressure distribution on sphere, at $M_\infty=15$ and $\gamma=1.4$ $R_{st} = 1.34$

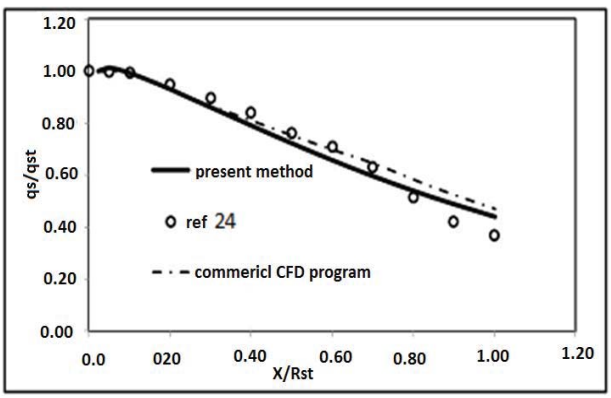

Fig. 9 Convection heating distribution on sphere at $T_W = 2.66'K$

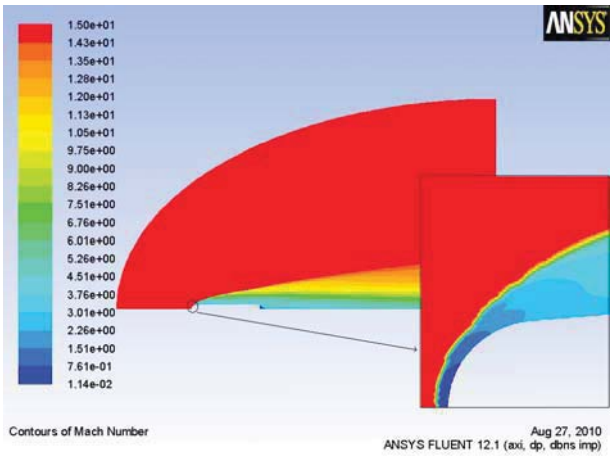

Fig. 10 Contours of Mach number for sphere at $M\infty=15$ and $\gamma=1.4$, $R_{st}=1.34$

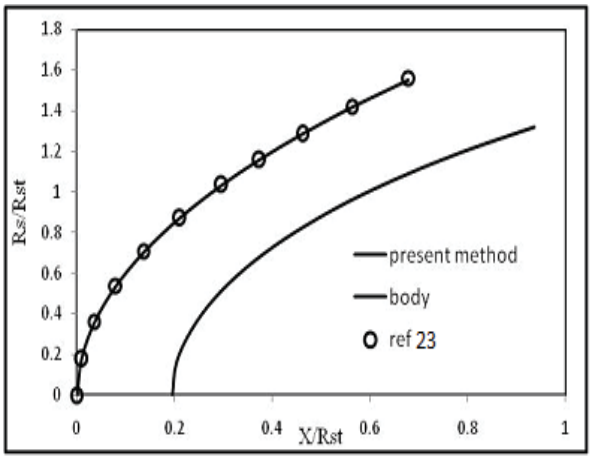

Fig. 12 Elliptic shock shape at $M_\infty=7$ and $\gamma=1.4$

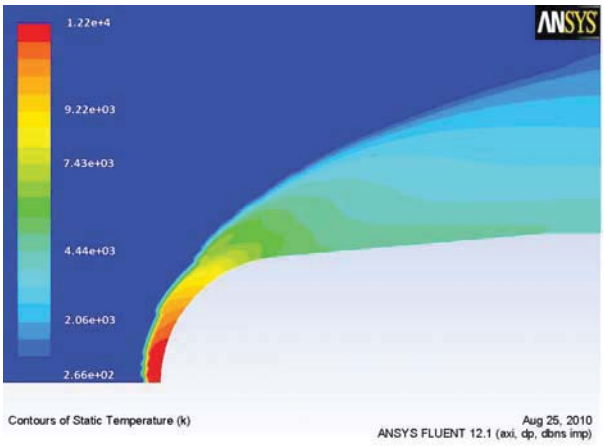

Fig. 11 Contours of temperature and contours of Mach number for sphere at $M\infty=15$ and $\gamma=1.4$, $R_{st}=1.34$

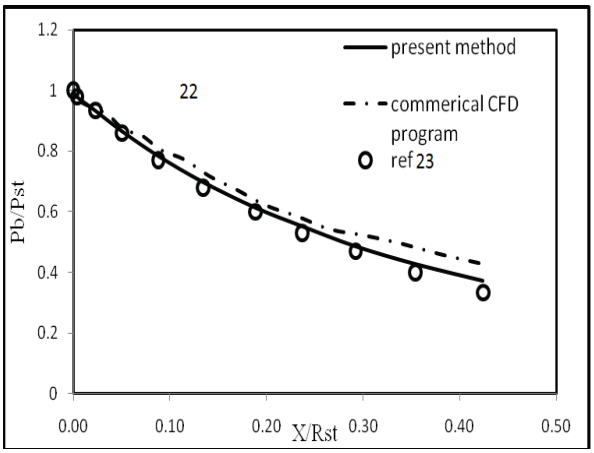

Fig. 13 Pressure distribution 0n 2/3 prolate ellipsoid at $M_\infty = 7$ and $\gamma = 1.4$, $a = 3$

In Figure 12, the shock shape over an elliptic blunted nose for M_∞ =7 and γ = 1.4 is illustrated. Moreover, the pressure distribution is shown in Figure 13. Reasonable results are obtained through the comparison between the present method and method of ref 23 (approximately 14%).

The convection heating rate over a ellipsoid blunted nose for M_∞ =7 and γ = 1.4 are shown in Figure 14; these results are compared with methods of ref 16 and 25 (the results of the comparison with ref 16 is approximately 15% and with ref 25 approximately10%). Fair agreement between the results of the present method and commercial CFD code data is shown in Figure 14 with differences less than 8%. Also temperature and Mach number contours are shown in Figures 15 and 16 which are related to commercial CFD program output results. The maximum q_{st} in Figure 4 is 49343.44 (MW/m^2).

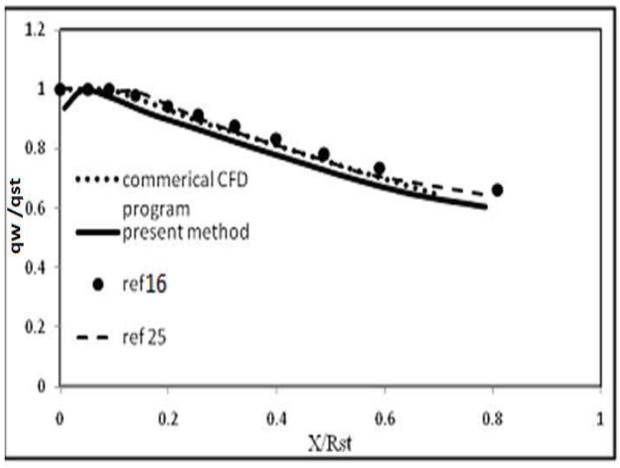

Fig. 14 Convection heating distribution on sphere at $T_W = 266'K$

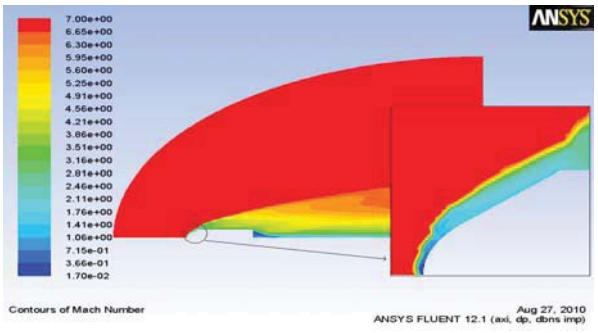

Fig. 15 Contours of Mach number for prolate ellipsoid at M∞=7 and γ=1.4, a=3

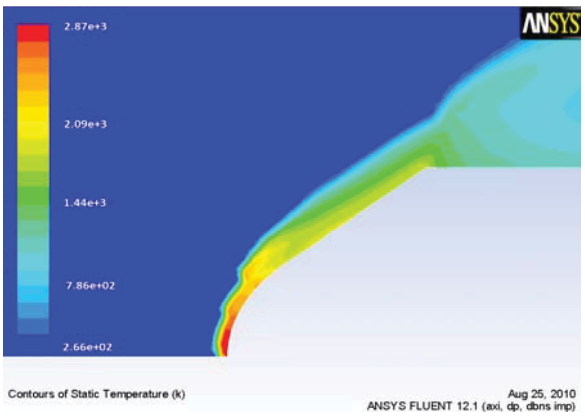

Fig. 16 Contours of Temperature for prolate ellipsoid at M∞=7 and γ=1.4, a=3

Conclusion

In this research aerodynamic heating around blunt nose reentry vehicle has been calculated. The results of the approximate methods are in good agreement with other researches. This method provides a rapid and at the same time reliable technique for prediction of convective- heating rates in parametric or design studies. Also increasing Mach number leads to the soar of the aerodynamic heating rate and the increase in the nose radius causes the aerodynamic heating rate to decrease.

References

[1] Shaw, C., Shan, Y.Y., Qin. N., "Development of a Local MQ-DQ-Based Stencil Adaptive Method and Its Application to Solve Incompressible Navier-Stokes Equations," *International Journal Number Method Fluids,* Vol. 55, Issue 4, 2007, pp. 367- 386.

[2] Shaw, C. and Qin, N., "Solution of the Navier-Stokes Equations for the Flow around an Aerofoil in Oscillating Free Stream," *Proceeding of the 20th Congress of the International Council of the Aeronautical Sciences*, ICAS, Vol. 1, 1996, pp.19-29.

[3] Lawrence, S. L, Chaussee. D. S. and Tannehill, J. C., "Application of an Upwind Algorithm to the Three-Dimensional Parabolized Navier-Stokes Equations," *AIAA paper 87-1112-CP*, June 1987.

[4] Birch, T., Prince. S., Ludlow, D. K. and Qin. N., "The Application of a Parabolized Navier-Stokes Solver to Some Hypersonic Flow Problems", *AIAA 2001-1753, 10th International Space Planes and Hypersonic Systems and Technologies Conference*, Kyoto, Japan, 2001.

[5] Esfahanian, V., Hejranfar, K. and Mahmoodi Darian, H., "Implementation of High-Order Compact Finite-Difference Method to Iterative Parabolized Navier-Stokes Equations," *Proceedings of the 25th International Congress of the Aeronautical Sciences*, ICAS2006, Hamburg, 2006.

[6] Miner, E. W. and Lewis, C. H., "Hypersonic Ionizing Air Viscous Shock-Layer Flows Over Nonanalytical Blunt Bodies," NASA CR-2550, 1975.

[7] Thompson, R. A., "Comparison of Nonequilibrium Viscous Shock-layer Solutions with Shuttle Heating Measurements," *Journal of Thermophysics and Heat Transfer*, Vol. 4, No. 2, 1990, pp. 162-169.

[8] Noori, S., Ghasemloo, S. and Mani, M., "A New Method for Solution of Viscous Shock Layer Equations," *Journal of Aerospace Engineering*, Vol. 224, part G, 2010.

[9] Noori, S., Karimian, S.M.H. and Malekzadehdirin, M., "Numerical Solution of Three-Dimensional Viscous Shock Layer Using Axisymmetric Analog the Streamlines," *International Journal of Numerical Methods for Heat & Fluid Flow*, Vol.18, No.1, 2008, pp. 36-49.

[10] Hamilton, H. H., Dejarnette, F.R. and Welmuenstrer, K.J., "Application of Axisymmetric Angle for Calculating Heating in Three-Dimensional Flows," *Journal of Spacecraft and Rockets*, Vol. 24, No. 4, 1987, pp. 296-302.

[11] Hamilton. H. H., Greene, F. A. and Dejarnette, F. R., "An Approximate Method for Calculating Heating Rates on Three-Dimensional Vehicles," *AIAA paper 93-2881*, 1993.

[12] Dejarnette, F. R. and Hamilton, H. H.,"Aerodynamic Heating on 3-D Bodies Including the Effects of Entropy-Layer Swallowing," *Journal of Spacecraft and Rockets*, Vol.12, No.1, 1975, pp. 5-12.

[13] Dejarnette, F. R. and Hamilton, H. H., "Inviscid Surface Streamlines and Heat Transfer on Shuttle-

Type Configurations," *Journal of Spacecraft and Rockets*, Vol.10, No.5, 1973, pp. 314-321.

[14] Zoby, E. V. and Simmonds, A. L., "Engineering Flow Field Method with Angle-of-Attack Applications", *Journal of Spacecraft and Rockets*, Vol. 22, No. 4, 1985, pp. 398-405.

[15] Hamilton, H. H., Greene, F. A. and Dejarnette, F. R., "Approximate Method for Calculating Heating Rates on Three-Dimensional Vehicles," *Journal of Spacecraft and rockets*, Vol. 31. No. 3, 1994, pp. 345-354.

[16] Riley, C. J. and Dejarnette, F. R., "Engineering Aerodynamic Heating Method for Hypersonic Flow," *Journal of Spacecraft and Rockets*, Vol. 29, No. 3, 1992, pp.327-339.

[17] Maslen, S. H., "Inviscid Hypersonic Flow Past Smoth Symmetric Bodies," *AIAA Journal*, Vol. 2, 1964, pp.1055-1061.

[18] Zoby, E.V., Moss, J.J. and Sutton, K., "Approximate Convective-Heating Equations for Hypersonic Flows," *Journal of Spacecraft and Rockets*, Vol. 18, No.1, 1981, pp. 64-70.

[19] White, F. M., *Viscous Fluid Flow*, McGraw-Hill Book Company, New York, USA, 1974.

[20] Dejarnette, F. R.,Hamilton, H. H., Weilmuenster, K. J. and Cheatwood, F.M., "A Review of Some Approximate Methods Used in Aerodynamic Heating Analysis," *Journal of Thermo Physics*, Vol. 1, No.1, 1978, pp. 5-12.

[21] Eckert, E. R. G., "Engineering Relations for Friction and Heat Transfer to Surfaces in High Velocity Flow," *Journal of the Aeronautical Sciences*, Vol. 22, No. 8, 1955, pp. 585-587.

[22]Van Dyke, M.D., Milton, D. and Gordon, H. D., "Supersonic Flow Past a Family of Blunt Axisymmetric Bodies," NASA TR R-1, 1959.

[23] Holt., M. and Hoffman Gilbert, H., "Calculation of Hypersonic Flow Past Sphere and Ellipsoids," *American Rocket Soc*., 61-209-1903, 1961.

[24] Mitcheltree, R. A., DiFulvio, M., Horvath, T. J. and Braun, R. D., "Aero Thermal Heating Predictions for Mars Microprobe," *Journal of Spacecraft and Rockets*, Vol. 36, No. 3 , pp. 405-411, 1999.

[25] Miller III, C. G., "Measured Pressure Distributions, Aerodynamic Coefficients, and Shock Shapes on Blunt Bodies at Incidence in Hypersonic Air and CF4," NASA TM-84489, 1982.